Journal of Catalysis **183,** 314–322 (1999)
Article ID jcat.1999.2435, available online at http://www.idealibrary.com on IDEAL®

H-Spillover and SMSI Effects in Paraffin Hydroisomerization over $Pt/WO_x/ZrO_2$ Bifunctional Catalysts

J. G. Santiesteban,[1] D. C. Calabro,[1] W. S. Borghard, C. D. Chang, J. C. Vartuli, Y. P. Tsao, M. A. Natal-Santiago,[2] and R. D. Bastian[3]

Mobil Technology Company, Strategic Research Center, Paulsboro, New Jersey 08066-0480

Received September 15, 1998; revised January 19, 1999; accepted January 20, 1999

The Pt-modified WO_x/ZrO_2 catalyst system is found to undergo various transformations in the presence of hydrogen. These transformations include the generation of spillover hydrogen at room temperature, the development of a strong Pt–W interaction at elevated temperatures, and tungsten reduction. We have characterized these effects using hydrogen chemisorption and temperature-programmed reduction techniques. We have also employed pentane isomerization as a test reaction to relate these changes to the acid catalysis of these materials. Our findings indicate that all of the above transformations are sensitive to tungsten loading. Room temperature hydrogen spillover is observed at 15.9 wt% tungsten, but is absent at tungsten loadings of $\leq$8.4 wt%. The higher tungsten loading catalyst exhibits a Pt–W SMSI effect in hydrogen at $>200^\circ$C; at lower tungsten loadings much higher temperatures are required to induce this effect. This result agrees with the increasing reducibility of tungsten oxospecies at higher loadings. Platinum greatly facilitates the tungsten reduction, is involved in a reversible Pt–W strong metal interaction, and likely enhances hydrogen spillover during pentane isomerization. By facilitating tungsten reduction, Pt can have a deleterious effect on the high acid activity of these WO_x/ZrO_2 catalysts.

Key Words: **modified zirconia; Pt-modified tungsten zirconia; hydrogen spillover; strong metal-support interaction; paraffin isomerization; dual functional catalysis.**

INTRODUCTION

The remarkable high activity exhibited by oxoanion-modified ZrO_2 materials for acid-catalyzed reactions has made them the focus of much research effort (1). The interest in these materials has increased lately and is driven by the need to replace liquid acids and halogen-containing solid acids. These acids are highly corrosive, are subject to stringent environmental regulations, and are difficult to handle and regenerate. Among the oxoanion-modified ZrO_2, SO_4^{-2}/ZrO_2-based materials have received the greatest attention because of their demonstrated high activity for the isomerization of *n*-butane at low temperatures (2, 3). However, the lack of long term stability and regenerability under commercial operating conditions are major limitations of this system.

The loss of acid activity of the SO_4^{-2}/ZrO_2-based catalysts has been attributed to the reduction of sulfur oxospecies (4, 5). Xu and Sachtler demonstrated that the reduction of the sulfate groups led to permanent partial sulfur loss from the catalyst surface (5). It has also been found that the presence of Pt enhances reduction of the sulfate groups and leads to the formation of H_2S, which not only results in the loss of acid sites but also deactivates the platinum (5–8).

Tungsten oxide supported on zirconia has been reported to exhibit high activity for acid catalyzed reactions and is presumably more stable toward over-reduction than the SO_4^{-2}/ZrO_2-based materials (9–13). The permanent loss of tungsten oxospecies due to over-reduction is not expected to take place in this system. The formation of stable, bifunctional catalysts by the addition of Pt to the highly acidic WO_x/ZrO_2 materials has recently been reported (14, 15).

Iglesia *et al.* showed that $Pt/SO_4^{-2}/ZrO_2$ and $Pt/WO_x/ZrO_2$ exhibited similar activity for low temperature (200°C) *n*-heptane isomerization, whereas at higher reaction temperature (250°C), $Pt/WO_x/ZrO_2$ was significantly more active (11). This was attributed to the greater stability of $Pt/WO_x/ZrO_2$ to deactivation by sublimation or decomposition of the acid sites at higher reaction temperatures. They also observed that $Pt/WO_x/ZrO_2$ has much higher isomerization selectivity than $Pt/SO_4^{-2}/ZrO_2$. This was attributed to loss of a hydrogen activating metal function due to sulfur poisoning of the Pt particles in $Pt/SO_4^{-2}/ZrO_2$ (8).

The traditional dual functional alkane isomerization pathway attributes a hydrogenation–dehydrogenation role to the metal (16, 17). Recent studies downplay this role and suggest that the ability of Pt to induce hydrogen activation

[1] To whom correspondence should be addressed.
[2] Current address: University of Wisconsin, Department of Chemical Engineering, Madison, WI 53706.
[3] Current address: Air Products and Chemicals, Inc., Allentown, PA 18195.

0021-9517/99 $30.00

and spillover may be its primary function (6, 11, 12, 18, 19). For example, the pentane hydroisomerization activity of a hybrid ($Pt/SiO_2 + USY$) catalyst shows no dependence on the dehydrogenation activity of the Pt (19). The capacity for Pt to catalyze the formation of spillover hydrogen is very sensitive to the nature of the support. Pt/ZrO_2 exhibits hydrogen spillover at 600°C (20), whereas room temperature is sufficient for Pt/MO_3 (21), and Pt/WO_3 (22, 23). Isotopic exchange experiments between *n*-heptane and deuterium indicates that $Pt/WO_x/ZrO_2$ is much more effective than $Pt/SO_4^{-2}/ZrO_2$ at activating and storing H-atoms. It has been suggested that this results in a longer residence time for surface carbocations on $Pt/SO_4^{-2}/ZrO_2$ resulting in more extensive cracking and reduced isomerization selectivity (11).

In the present work, we describe studies of $Pt/WO_x/ZrO_2$ and Pt-free WO_x/ZrO_2 catalysts which reveal that tungsten oxospecies are also susceptible to a partial loss of high acid activity due to hydrogen exposure at moderate reaction temperatures (>250°C, 350 psig). Our studies also indicate a large reversible loss of hydrogen chemisorption capacity on the $Pt/WO_x/ZrO_2$ catalyst with increasing pretreatment temperature. Both high acid activity and hydrogen chemisorption capacity of the hydrogen reduced $Pt/WO_x/ZrO_2$ catalysts can be restored by oxidation treatments. In addition, $Pt/WO_x/ZrO_2$ is found to generate large amounts of spillover hydrogen at ambient conditions.

EXPERIMENTAL

Catalyst Preparation

WO_x/ZrO_2 catalysts with different W loading were prepared by the coprecipitation method as described earlier (13). Briefly, an alkaline slurry (pH 9) containing $ZrOCl_2 \cdot 8H_2O$, ammonium metatungstate and ammonium hydroxide was heated to ~100°C for 72 h. The product was filtered, washed with excess water, dried overnight at 95°C, and calcined in flowing air at 825°C for 3 h. Pt was added to the mixed oxide via incipient wetness using an 8 wt% H_2PtCl_6 solution; the final catalyst was air dried at 120°C for 2 h and then air calcined at 300°C for 2 h. The elemental composition and BET surface area of the different catalysts used in this study are given in Table 1.

TABLE 1

Catalyst Composition and BET Surface Area

Catalyst	Concentration (wt%) W	Zr	Pt	BET (m^2/g)
$Pt/WO_x/ZrO_2$	15.9	58.6	0.67	64
$Pt/WO_x/ZrO_2$	8.4	60.4	0.63	61
WO_x/ZrO_2	1.9	—	—	32
Pt/ZrO_2	—	—	0.51	10

Characterization

Hydrogen chemisorption apparatus and procedure. Initial chemisorption measurements were made on an automated volumetric apparatus. Following sample pretreatment (see Appendix) on the unit, the sample was cooled to room temperature in vacuum, and hydrogen uptake was determined at ten dose pressures in the range of 10–400 Torr. The equilibration time for each point was preset, based upon previous experience with other Pt systems: 30 min for the first point, 20 min for the next four, and 10 min for the last five. The resultant isotherm was extrapolated to zero pressure to determine the monolayer coverage of chemisorbed hydrogen atoms per Pt atom. Repeat isotherms were not performed.

Measurements on a given catalyst were all performed on a single sample (3–5 g) using a 60-h program of alternating pretreatment and hydrogen chemisorption sequences. The room temperature hydrogen chemisorption was measured as a function of prereduction temperature. The effect(s) of high temperature oxidation on subsequent hydrogen chemisorption was also determined.

Spillover measurements were done on a Micromeritics ASAP-2010C. Pretreatment consisted of drying in helium at 150°C, reducing in H_2 at 250°C, and evacuation at 250°C, each for 30 min. The isotherms were measured at 35°C from 1 to 760 Torr.

Temperature-programmed reduction. Temperature-programmed reduction (TPR) studies were carried out by monitoring weight changes during reduction using a DuPont 9000 Thermal Analyzer with a 951 TGA module. Calibration of the TGA was performed using the decomposition of calcium oxalate ($CaC_2O_4 \cdot H_2O$). The mass of the samples was recorded as a function of temperature during the reduction. In all of the experiments, the temperature was increased at a linear rate of 6°C/min from 30 up to 1000°C. In typical experiments, 40–70 mg of fine powder were contained in a quartz pan for the reduction reaction. Hydrogen flow rate was 100 cc/min while that of the balance's purge gas, nitrogen, was 25 cc/min. To remove any adsorbed species such as water prior to the analyses and to ensure a full state of oxidation for tungsten, the samples were calcined in air at 600°C for 60 min. The reduction data were collected in the form of mass and rate of mass loss (Rm) profile versus temperature.

X-ray diffraction. The X-ray diffraction (XRD) data were collected using Cu $K\alpha$ radiation on a Scintag XDS2000 diffraction system equipped with a lithium-drifted germanium solid state detector. The diffraction data were recorded by step-scanning at 0.04° 2θ per step and a counting time of 2 s per step.

Catalytic Testing

Catalytic studies were carried out in a down-flow fixed-bed stainless-steel reactor. Catalyst samples were crushed and sieved to retain 14/30 mesh particle size. Prior to testing, the catalysts were pretreated at 500°C in flowing dry air for 1 h at atmospheric pressure to remove adsorbed water and/or adventitious carbon. After catalyst pretreatment, the reactor was cooled to ambient temperature and the unit was pressurized with hydrogen (Matheson, UHP) to 350 psig. Hydrogen was passed through a catalytic purifier and a 13X sieve trap before use. *n*-Pentane (Aldrich, >99%) was fed into the reactor using a high pressure ISCO pump. Hydrogen and *n*-pentane flow rates were adjusted to give a 2 H_2/n-C_5 mol ratio. The temperature was then gradually increased to the desired operating temperature. After depressuring via a backpressure regulator, the reactor effluent was diluted with nitrogen, and the combined stream was sent to on-line gas chromatography sampling for analysis. A fused silica capillary column (DB-1, 60 m) run isothermally at 20°C was used to determine product composition.

RESULTS AND DISCUSSION

$Pt/WO_x/ZrO_2$ is susceptible to various related, hydrogen-induced transformations. These include the extent of metal (both Pt and W) reduction under pretreatment and reaction conditions, the generation of spillover hydrogen (see above), and the presence of a strong metal–support interaction. All of these factors affect the acid and/or metal function of this catalyst and therefore greatly impact its performance.

In addition to metal dispersion, hydrogen chemisorption can also indicate the presence of spillover and SMSI effects. Since the extent of metals reduction is important, we have measured hydrogen chemisorption as a function of prereduction temperature. We have combined this with temperature programmed reduction data to obtain a better understanding of the hydrogen-sensitivity of this catalyst.

Hydrogen Chemisorption on WO_x/ZrO_2-based Catalysts

All of the reported H/Pt ratios were determined at 30°C following elevated temperature prereduction and evacuation. When oxygen pretreatment was employed, it was always followed by a hydrogen reduction at 200°C and evacuation, prior to the room temperature hydrogen chemisorption measurement. Therefore, any hydrogen uptake due to either the reduction of metals or the creation of spillover hydrogen during high temperature prereduction is not included in these measurements. The Pt-free WO_x/ZrO_2 possessed no hydrogen chemisorption even after a 450°C prereduction. With the possible exception of room temperature generated hydrogen spillover (e.g., Pt/WO_3 (22)), the measured H/Pt ratio should solely reflect the available Pt surface area.

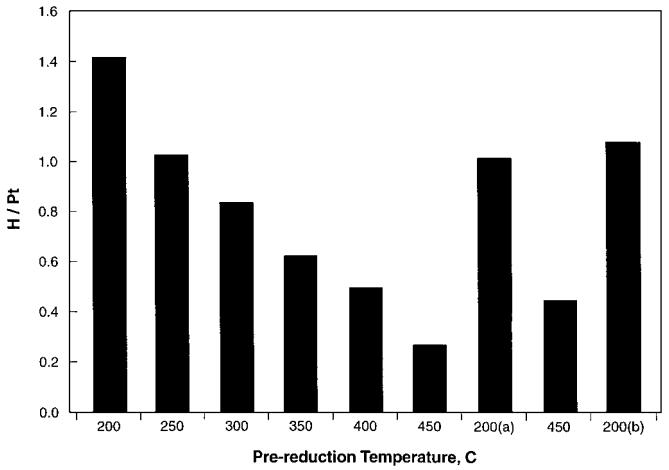

FIG. 1. Hydrogen chemisorption (H/Pt) as a function of prereduction temperature for $Pt/WO_x/ZrO_2$ (15.9 wt% W). Preceded by oxidation at (a) 350°C and (b) 450°C.

H/Pt versus reduction temperature for $Pt/WO_x/ZrO_2$ (15.9 wt% W) is plotted in Fig. 1. The H/Pt ratio of 1.4 following the initial 200°C reduction indicates highly dispersed Pt. An H/Pt value in excess of 1 has been observed by many other researchers in various systems and is usually attributed, in the absence of significant hydrogen spillover, to a surface chemisorption stoichiometry of 2 for the hydrogen adsorbate on the corner and edge atoms of very small metal particles. As reduction temperature is increased in 50°C increments, the measured H/Pt ratio decreases continuously, reaching a value of 0.28 following reduction at 450°C. While a decrease in H/Pt ratio is most often attributed to Pt agglomeration, this is found not to be the case here based on the effect of oxygen pretreatment. Reoxidation of the 450°C reduced sample at 350°C in oxygen, followed by reduction at 200°C, increased H/Pt to 1.02 (third data point from the right in Fig. 1). The reversibility of these H/Pt changes is further demonstrated in the last two data points where reduction at 450°C again decreases H/Pt (0.45), which is again restored to 1.09 by 450°C oxidation followed by 200°C reduction. If the decline in H/Pt with increasing reduction temperature had been due to Pt agglomeration, simple exposure to oxygen at 350°C would not reverse it.

The above chemisorption behavior can be attributed to a classical SMSI-type effect (24–26). The strong metal-support interaction occurs via the partial reduction of the support by activated (spillover) hydrogen. For most systems, the spillover of hydrogen from the Pt to the support is the rate-determining step (27). In Pt/ZrO_2, SMSI can involve Pt decoration with partially reduced zirconium oxide, ZrO_{2-x} and/or Pt–Zr alloy formation during elevated temperature reduction (20, 28–30). However, the latter is generally observed at significantly higher temperatures than those shown in Fig. 1. In $Pt/WO_x/ZrO_2$, SMSI effects might

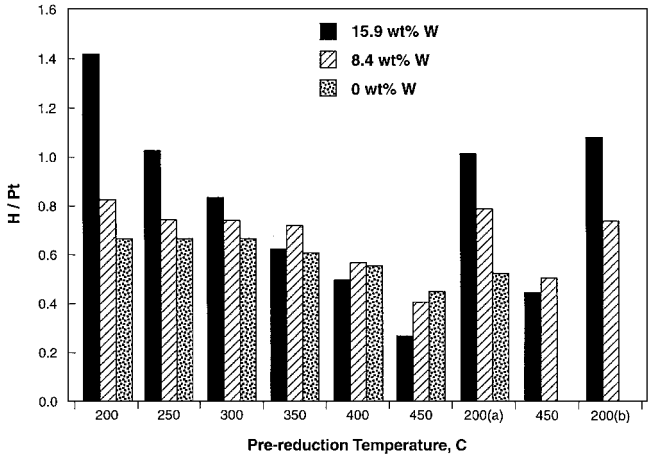

FIG. 2. Hydrogen chemisorption (H/Pt) versus prereduction temperature for $Pt/WO_x/ZrO_2$ as a function of tungsten loading. Preceded by oxidation at (a) 350°C and (b) 450°C.

TABLE 2

Hydrogen Chemisorption as a Function of Pretreatment Gas and Temperature for ZrO_2-Supported Pt Catalysts

Pretreatment, deg. C		H/Pt		
O_2	H_2	15.9% W	8.4% W	0% W
	200	1.41	0.82	0.66
	250	1.03	0.74	0.67
	300	0.84	0.74	0.67
	350	0.63	0.72	0.61
	400	0.50	0.57	0.56
	450	0.28	0.41	0.45
350	200	1.02	0.79	0.53
	450	0.45	0.51	n.m.
450	200	1.09	0.74	n.m.

also result from Pt decoration by reduced WO_x species, especially in light of the facile propensity of WO_3 to undergo reduction by spillover hydrogen (23, 31). If so, the observed chemisorption reduction temperature dependence should be sensitive to the tungsten reducibility.

Figure 2 compares the hydrogen chemisorption reduction temperature dependence for $Pt/WO_x/ZrO_2$ catalysts having tungsten loadings of 15.9, 8.4, and 0 wt%. A significant tungsten loading effect on the extent of H/Pt decline with increasing reduction temperature is observed. As the reduction temperature is increased from 200 to 450°C, all three catalysts eventually exhibit a decrease in H/Pt. The 15.9 wt% W catalyst shows decreasing H/Pt ratios over the entire reduction temperature range, whereas the 8.4 wt% W and 0 wt% W catalysts exhibit little or no loss in hydrogen chemisorption at reduction temperatures as high as 350°C. After reduction at 450°C, all three catalysts have H/Pt ratios of ~0.3–0.5, with the Pt/ZrO_2 catalyst retaining the highest value (0.45). Thus, the extent of chemisorption loss with increasing reduction temperature increases with the W loading of the catalyst.

The results given in Fig. 2 and Table 2 also show that all three catalysts undergo significant hydrogen chemisorption recovery following high temperature oxidation–low temperature reduction treatment. As stated above, we attribute this to a reversal of the strong metal–support interaction which develops under high temperature reducing conditions. Nonetheless, none of the catalysts recover all of the chemisorption capacity of the initial 200°C reduction data point. In the absence of additional data, we attribute this to either a small amount of irreversible Pt decoration by WO_x or a modest degree of Pt agglomeration during the sequential, variable temperature measurements, or both. This residual, unrecovered chemisorption is largest for the 15.9% W catalyst. As we will show below, variation in the capacity for generating room temperature hydrogen spillover may also have a role in this irreversible chemisorption loss.

The observed SMSI effects in Fig. 2 are most pronounced in the 15.9 wt% W catalyst. Coupled with the modest SMSI effects observed on Pt/ZrO_2 at these reduction temperatures (20, 29, 30), we attribute the loss of hydrogen chemisorption in $Pt/WO_x/ZrO_2$ primarily to the formation of a strong Pt–W interaction, where W exists as a reduced or partially reduced (WO_x, where $0 < x < 3$) surface species. The sensitivity to W loading can be explained by the relative reducibility of supported tungsten oxospecies, as discussed below.

Temperature-Programmed Reduction of WO_x/ZrO_2

The TPR profiles of Pt-free WO_x/ZrO_2 catalysts containing different W loadings are presented in Fig. 3 along with those obtained on bulk WO_3 and ZrO_2. The zirconia

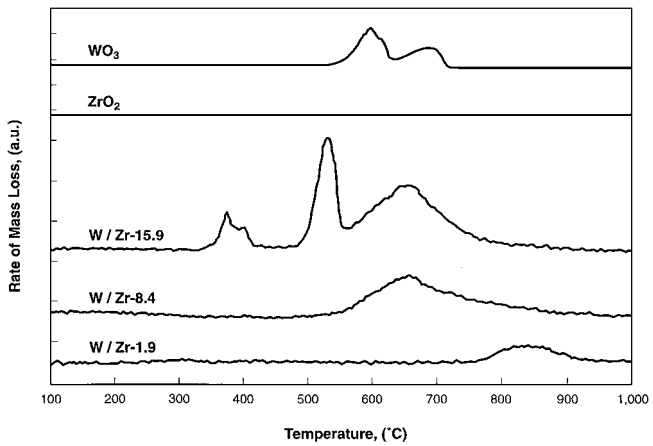

FIG. 3. Temperature programmed reduction profiles for WO_3, ZrO_2, and three WO_x/ZrO_2 materials having tungsten loadings of 15.9, 8.4, and 1.9 wt%.

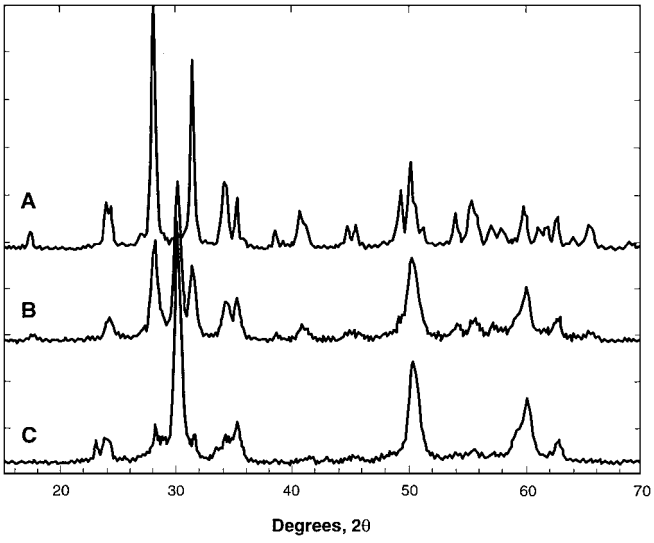

FIG. 4. X-ray diffraction patterns for WO_x/ZrO_2 materials having tungsten loadings of (A) 1.9 wt%, (B) 8.4 wt%, and (C) 15.9 wt%.

support undergoes no detectable reduction at temperatures as high as 1000°C; therefore the profiles in Fig. 3 are attributed to the reduction of supported WO_x. The data indicates that as tungsten loading increases, the reduction peak shifts to lower temperature until the stepwise reduction of bulk WO_3 is observed in the WO_x/ZrO_2 material containing 15.9 wt% W. The X-ray diffraction patterns of the same three WO_x/ZrO_2 materials are shown in Fig. 4. The 15.9% W sample shows a peak at ~22.8° 2θ which can be attributed to the presence of bulk WO_3. This peak is absent in the lower tungsten loading samples.

The reducibility of tungsten oxospecies as a function of loading level is well documented (11, 32). Generally, at less than monolayer coverage, tungsten oxospecies are difficult to reduce due to a strong WO_x–support interaction (33–36). In the case of WO_x/ZrO_2, monolayer coverage corresponds to ca. 7 wt% W (assuming WO_4^{-2}). Thus, the WO_x/ZrO_2 sample containing 1.9 wt% W in Fig. 3 exhibits a broad reduction peak with a maximum at about 810°C, at 8.4 wt% W this becomes a broad asymmetric peak with a maximum at about 610°C, and finally, two major peaks with maxima at about 525 and 655°C, and two minor peaks in the 350–410°C range, are observed at 15.9 wt% W. It should be mentioned that the intensity of these smaller peaks varied considerably from run to run, and therefore they should only be considered from a qualitative viewpoint. However, it should also be emphasized that these low temperature peaks were never observed in the samples containing 1.9 and 8.4 wt% W. These minor low-temperature reduction peaks observed at the 15.9 wt% tungsten loading were also observed by Iglesia *et al.* on WO_x/ZrO_2 catalysts containing 21 wt% W, but not on catalysts containing 7.9 and 2.2 wt% W (11). In addition, they found that the introduction of Pt only weakly influenced the two high-temperature reduction peaks, but markedly decreased the temperature of the low-temperature peaks from 427 to 77°C. Finally, X-ray absorption near-edge spectroscopy (XANES) studies of $Pt/WO_x/ZrO_2$ containing 12 wt% W indicated that partial tungsten reduction took place during reduction pretreatment at 350°C (12).

The TPR results described above are entirely consistent with the chemisorption results in Fig. 2. As tungsten loading increases, it becomes easier to reduce the supported WO_x species and the onset of SMSI-type Pt decoration occurs at a lower reduction temperature.

The Determination of Spillover Hydrogen in $Pt/WO_x/ZrO_2$

As stated above, the capacity for Pt to generate spillover hydrogen may play an important role in these modified zirconia-based catalysts. Returning to Fig. 2, we note a large difference in the measured H/Pt ratio of the three catalysts when prereduced at 200°C. While it might be possible for tungsten loading to impact Pt dispersion, variable degrees of room temperature hydrogen spillover could also explain these observations. Recall that the TPR results in Fig. 3 indicated that 15.9% WO_x/ZrO_2 possessed reduction peaks suggesting the presence of bulk WO_3. Since Pt/WO_3 is known to generate spillover hydrogen at room temperature (22), this could significantly contribute to the much higher H/Pt ratio of the 15.9% WO_x/ZrO_2 catalyst.

Utilizing a second device to measure chemisorption wherein the adsorption system was allowed to equilibrate for as long as necessary, new results emerged. Table 3 presents equilibrated hydrogen uptake results for two

TABLE 3

Equilibrium Hydrogen Uptake for $Pt/WO_x/ZrO_2$ at Two Pt Loadings

		2 g sample			1 g sample		
wt% W	wt% Pt	H/Pt	cm^3/g	Time to 1st point (hh : mm)	H/Pt	cm^3/g	Time to 1st point (hh : mm)
15.9	0.51	1.8	0.54	6 : 40	2.0	0.60	7 : 08
15.9	0.07	1.8	0.07	2 : 17	1.6	0.06	0 : 51
8.4	0.30	—	—	—	0.8	0.15	1 : 08
0	0.41	—	—	—	1.0	0.24	0 : 39

samples of 15.9% WO_x/ZrO_2 containing different Pt loadings as well as Pt/8.4% WO_x/ZrO_2, and Pt/ZrO_2.

The high tungsten loading, 0.51% Pt sample required unusually long equilibration times (6–7 h) as illustrated by the time to stabilize at the first isotherm dose pressure. Presumably, it could take days to fully equilibrate with a more stringent criterion. Furthermore, the H/Pt ratios for both of the high tungsten samples were above 1.5, which is the highest value that we had ever measured. The H/Pt did not change much as a function of Pt loading, whereas the total sorption per gram (cm^3/g) increased linearly. From this, one might deduce that H only sorbs on the Pt; however, the other observations (time and H/Pt) are rather compelling.

The 8.4 and 0% tungsten samples have more typical values for the H/Pt ratio, and the equilibration times to the first isotherm point are low. Also, the total sorption is proportionately much lower relative to Pt loading than was observed for the 15.9% tungsten samples.

From these observations, we conclude that hydrogen spillover is taking place on the high tungsten loading Pt/WO_x/ZrO_2 catalyst at room temperature. This is consistent with the presence of bulk-like WO_3 suggested in the TPR and XRD results shown above and the known propensity of Pt/WO_3 to form spillover hydrogen at room temperature. At high spillover coverages, hydrogen may adsorb on and spillover from the WO_3 bronze (31). This, however, does not change the conclusion.

The presence of room temperature hydrogen spillover in the high tungsten loading sample and its absence in the lower tungsten and tungsten-free samples provides a ready explanation for the observed differences in H/Pt of these samples following 200°C reduction (Fig. 2). The H/Pt ratios in Fig. 2 consist of a major contribution due to conventional hydrogen chemisorption which is susceptible to the SMSI effects described above and, in the case of the 15.9% W sample, a minor contribution from room temperature spillover hydrogen uptake. At least part of the much higher H/Pt ratio observed for the 15.9% W sample can be attributed to this second contribution which is absent in the other samples. We can speculate that the partial, irreversible loss of chemisorption, which was highest for the 15.9% tungsten sample, may be due to extensive dehydration of the WO_x/ZrO_2 surface via the 200°C evacuation prior to each high temperature reduction (see Appendix). Since the presence of water is known to play a critical role in generating spillover hydrogen tungsten bronze at room temperature (37, 38), this contribution to the measured H/Pt ratio is thereby lost, and the oxygen regenerations only restore the traditional hydrogen chemisorption of the available Pt surface area.

Catalytic Activity Data

The above results illustrate the various hydrogen-induced transformations which can take place on WO_x-modified zirconia. Under pretreatment or reaction conditions where these effects are operative, the WO_x surface structure, and therefore the acidity and catalytic activity of these materials, could be impacted. Earlier we employed pentane isomerization as a test reaction for the acid activity of Pt-free WO_x/ZrO_2 (13). We have now measured the pentane isomerization activity of Pt-containing WO_x/ZrO_2 (15.9 wt% W) after hydrogen pretreatments at 200 and 350°C. The results are shown in Table 4. The steady state isomerization data in Table 4 were interpreted kinetically in terms of a reversible first-order reaction, for which the integrated rate expression is

$$k_A = (1/t)(\mathrm{Xe})[-\ln(1 - X/\mathrm{Xe})],$$

where Xe is the equilibrium conversion, $1/t$ is the space velocity in molecules of n-C_5 feed/cm^2 of catalyst · s, and k_A is the forward areal rate constant in molecules of n-C_5 isomerized/cm^2 of catalyst · s. The equilibrium conversion at 200°C was calculated to be 74.8% i-C_5/total C_5's.

Comparison of the catalyst activity after it was pretreated in hydrogen at 200 vs 350°C clearly revealed that the higher temperature pretreatment caused a loss in catalytic activity. Based on the decrease in k_A, approximately 75% of the strong acid sites of Pt/WO_x/ZrO_2 (15.9 wt% W) have lost their activity following the 350°C hydrogen pretreatment. Interestingly, as with the observed loss of hydrogen chemisorption, the high isomerization activity of the catalyst was fully restored by air calcination at 350°C (third data column in Table 4). Recalling the data in Fig. 1, both the extent and reversibility of the SMSI-induced chemisorption loss is matched by a concomitant loss in pentane isomerization activity for the 15.9 wt% W Pt/WO_x/ZrO_2 catalyst.

TABLE 4

Effect of Hydrogen Temperature Pretreatment on the Pentane Isomerization Activity of Pt/WO_x/ZrO_2 (15.9 wt% W)

Pretreatment			
Gas[a]	Hydrogen	Hydrogen	Air[b]
Temperature (°C)	200	350	350
Time (hrs)	2	2	1
Product distribution (wt%)			
Cracking products, C_4-.	2.4	0.4	2.5
i-C_5H_{12}	70.8	46.1	71.1
n-C_5H_{12}	25.8	53.4	25.6
C_6's	0.9	0.1	0.8
i-C_5/total C_5's	73.3	46.3	73.5
Forward areal rate constant (k_A)	10.2×10^{12}	2.5×10^{12}	10.5×10^{12}

Note. Reaction conditions were 200°C, $2H_2/n$-C_5 molar ratio, 2 LHSV (ml n-C_5/ml cat · h), and 350 psig.

[a] Pretreatment was carried out at ambient pressure, GHSV = 1500 h^{-1}.

[b] High activity of the catalyst reduced at 350°C is restored by air oxidation at 350°C. No hydrogen pretreatment was used during this run.

TABLE 5

Effect of High Reaction Temperature on the Acid Activity of WO_x/ZrO_2 (15.9 wt% W)

Reaction temperature (°C)	232	260	232	232[a]
Product distribution (wt%)				
CH_4	0.3	0.3	0.3	0.3
C_2H_6	0.8	0.7	0.8	0.6
C_3H_8	2.6	10.4	1.0	2.1
i-C_4H_{10}	17.2	35.0	3.9	14.9
n-C_4H_{10}	1.1	4.0	0.4	0.8
i-C_5H_{12}	55.5	33.2	66.9	56.3
n-C_5H_{12}	20.3	12.8	25.6	22.2
C_6's	2.2	3.6	1.0	2.8
Total cracking products C_4- (wt%)	22.0	50.4	6.5	18.7

Note. Reaction conditions were $2H_2/n$-C_5 molar ratio, 2 LHSV (ml n-C_5/ml cat · h), and 350 psig.

[a] Preceded by air calcination at 500°C, 1500 GHSV, 1 h.

We reported earlier that the strong acid site density of the WO_x/ZrO_2 catalyst prepared by coprecipitation was about 0.004 meq H^+/g catalyst (13). The results in Table 4 suggest that exposure to hydrogen at 350°C decreases the concentration of strong acid sites to only about 0.001 meq H^+/g catalyst.

Under high pressure reaction conditions, even lower temperatures than shown in Fig. 3 can cause a decrease in the acid activity of Pt-free WO_x/ZrO_2. This is illustrated in Table 5. For these experiments a Pt-free WO_x/ZrO_2 catalyst containing 15.9 wt% W was used. The data presented in Table 5 were obtained by initially testing the catalyst, without hydrogen pretreatment, at 232°C for 15 h, then the temperature was increased to 260°C and maintained there for about 24 h. Subsequently the temperature was lowered back to 232°C to determine the activity of the catalyst after exposure to 260°C. The last data column was obtained after regeneration of the catalyst with air at 500°C for 1 h. At both 232 and 260°C, the *n*-pentane to isopentane isomerization reaction is at thermodynamic equilibrium, thus, we used the yields of cracking products, C_4-, to monitor the acid activity of the catalyst. It should be noted that the cracked products distribution indicates that these products are mainly formed via oligomerization-β scission processes involving carbenium ion chemistry, i.e., acid catalysis. This is clearly reflected, for example, by the higher selectivity of isobutane compared to *n*-butane. Carbenium ion chemistry favors the formation of tertiary fragments, precursors of isobutane, over the formation of secondary or primary fragments, precursors of *n*-butane (39, 40).

The data of Table 5 clearly indicated that the acid activity of the WO_x/ZrO_2 catalyst, as determined by the yields of cracking products, C_4-, decreased after the reaction temperature was increased to 260°C. As with $Pt/WO_x/ZrO_2$ (Table 4), the initial activity was almost entirely restored by oxidation at 500°C. Temperature-programmed experiments performed on catalysts after being tested at 260°C indicated the absence of coke. We can only speculate that even though this temperature is still 115°C cooler than the lowest temperature TPR peak for WO_x/ZrO_2, the loss in cracking activity of this catalyst may be due to the detrimental, high pressure-induced, reduction of some fraction of the active tungsten oxospecies.

The above catalytic and characterization results can be interpreted to gain a better understanding of the nature of the active site in the WO_x/ZrO_2 catalyst. It has been observed that tungsten loadings well in excess of one monolayer are required to achieve high acid activity in WO_x/ZrO_2 (9, 11, 13). We have also shown that both the presence of low temperature reduction peaks in the TPR and the ability to generate room temperature spillover hydrogen require comparably high tungsten loadings. It is pertinent to ask how these factors relate to catalytic activity.

At the tungsten loadings necessary for high acid activity, low temperature reducible tungsten oxospecies are also present in the catalyst. This coexistence does not necessarily indicate that the active site contains reduced tungsten species. This could only be the case if the catalyst were exposed to hydrogen during pretreatment or reaction conditions which were sufficient to affect this low temperature tungsten reduction. Based on the TPR results presented here and elsewhere, this is the case in $Pt/WO_x/ZrO_2$ containing a high tungsten loading where, assuming the lowest temperature peak (77°C) (11) is due to the reduction of tungsten and not Pt, is much lower than typical pentane isomerization reaction temperatures (130–260°C). However, in the absence of Pt the lowest tungsten reduction temperature of ~375°C (see Fig. 3) is much higher than the reducing temperatures which the catalyst is ever exposed to during pentane isomerization. Nevertheless, we have obtained equilibrium pentane isomerization over Pt-free 15.5% WO_x/ZrO_2 which has never been exposed to hydrogen at higher than reaction temperature (210°C) (13). As discussed above, the results in Table 5 indicate the loss of activity by exposure to high pressure hydrogen at 260°C which could be due to tungsten oxospecies reduction. Nonetheless, in the absence of data establishing tungsten reduction under high pressure, high activity conditions, there is no reason to assume that the delta between the reaction temperature (210°C) and the lowest temperature TPR reduction peak (375°C) is overcome and that the highly active Pt-free catalyst contains anything other than fully oxidized tungsten. The determination of tungsten reducibility in high pressure hydrogen is needed to clarify this issue.

Therefore, while the connection between tungsten reducibility, the onset of SMSI effects, and the loss of catalytic activity is clear, there is no conclusive evidence connecting the active tungsten oxospecies to an optimum intermediate

tungsten oxidation state. The enhanced tungsten reducibility in the presence of Pt does not result in increased pentane isomerization activity. Even though the low temperature reducible tungsten species have likely undergone some degree of reduction under reaction conditions in $Pt/WO_x/ZrO_2$ containing 15.9 wt% W, the likelihood that these same species are unreduced in the Pt-free catalyst with no associated loss in activity suggests that tungsten reduction is not a prerequisite for activity.

A relationship between hydrogen spillover and catalytic activity has also been suggested (6, 11, 12, 18, 19). It is proposed that spillover hydrogen diffuses to Lewis acid sites in WO_x/ZrO_2, where it donates an electron to generate a proton (Brønsted site). While our observation of room temperature hydrogen spillover only in the high tungsten loading $Pt/WO_x/ZrO_2$ is consistent with its high activity, the equally active Pt-free WO_x/ZrO_2 again must be noted. The generation of hydrogen spillover is generally attributed to a metal function. While a stationary rate of hydrogen insertion can be maintained at room temperature on "activated" MO_3 ($M =$ Mo, W) in the absence of Pt, the activation requires a source of atomic hydrogen which is provided by supported Pt (31). Therefore, since the Pt-containing and Pt-free catalysts exhibit comparable acid activity, we conclude that hydrogen spillover does not play a crucial role in acid site formation in this system.

CONCLUSIONS

The $Pt/WO_x/ZrO_2$ catalyst undergoes a reversible loss of hydrogen chemisorption capacity with increasing hydrogen pretreatment temperature. The temperature at which this effect is observed is sensitive to the tungsten loading and was shown to correlate with increased tungsten reducibility. This loss in accessible Pt surface area is mostly attributed to the presence of a strong Pt-reduced tungsten oxospecies interaction (SMSI) and to a much lesser extent, if any, to ZrO_2 species. Oxidation at 350°C restores most of the hydrogen chemisorption capacity. A small amount of irreversible hydrogen chemisorption loss is also observed, especially in the high tungsten loading (15.9 wt%) WO_x/ZrO_2 catalyst.

The above chemisorption changes were accompanied by a reversible loss of pentane isomerization activity. The loss of high acid activity in the WO_x/ZrO_2-based catalysts due to reduction of the tungsten oxospecies is reversible. High acid activity is restored with mild oxidation treatments, for example 350°C.

It is proposed that low-temperature reducible tungsten oxospecies present in $Pt/WO_x/ZrO_2$ containing about 16 wt% W are responsible for the loss of hydrogen chemisorption capacity. Ambient pressure TPR data suggest that these low temperature reducible tungsten oxospecies have likely undergone some degree of reduction at pentane isomerization conditions in the $Pt/WO_x/ZrO_2$ (~16% W) catalyst, but that this may not be the case in the less reducible, Pt-free WO_x/ZrO_2. High pressure, *in situ* characterization of this system under actual catalytic conditions is required to conclusively determine the tungsten oxidation state of the active catalyst. However, one must keep in mind that the number of active sites are very small in this system and may be difficult to distinguish from spectator WO_x sites (13).

Room temperature hydrogen spillover is observed in the $Pt/WO_x/ZrO_2$ (~16% W) catalyst, consistent with the presence of bulk WO_3 in this material as observed by TPR. The lower tungsten loading (8.4%) $Pt/WO_x/ZrO_2$ and Pt/ZrO_2 materials show no evidence of spillover hydrogen generation at room temperature.

APPENDIX

Sample pretreatments prior to the initial chemisorption measurements were done using these procedures.

Prereduction Procedure

1. Evacuate sample via roughing pump at room temperature for 5 min.
2. Heat to 200°C under roughing vacuum, hold for 5 min (drying step).
3. Evacuate under high vacuum via Hg diffusion pumps for 20 min.
4. Dose sample with 250 Torr hydrogen.
5. Heat to desired prereduction temperature, hold 30 min.
6. Collect and measure remaining hydrogen.
7. Evacuate at prereduction temperature for 30 min or until outgassing rate <0.4 mtorr/min.

Sequential Oxidation–Reduction Pretreatment Procedure

1. Repeat step 1 above.
2. Heat to desired oxidation temperature under roughing vacuum, hold for 5 min.
3. Repeat step 3 above.
4. Dose sample with 250 torr oxygen, maintain at oxidation temperature for 30 min.
5. Collect and measure remaining oxygen.
6. Evacuate at oxidation temperature for 30 min.
7. Reset temperature to 200°C.
8. Dose 250 torr hydrogen at 200°C.
9. Heat to desired prereduction temperature under hydrogen, hold 30 min.
10. Collect and measure remaining hydrogen.
11. Evacuate at prereduction temperature for 30 min or until outgassing rate <0.4 mtorr/min.

Hydrogen Chemisorption Procedure

1. Repeat step 11 above.

2. Reset temperature to 30°C.
3. Evacuate for 3 min.
4. Measure hydrogen uptake at 10 dose pressures spaced within the range of 10–400 torr.

ACKNOWLEDGMENTS

The authors appreciate the assistance of Douglas Colmyer in the collection of the chemisorption data and Mobil Technology Company for supporting this research.

REFERENCES

1. Arata, K., *Adv. Catal.* **37**, 165 (1990).
2. Hollstein, Wei, Hsu, U.S. Pat. 4,918,941, assigned to Sun Refining and Marketing Co., 1990.
3. Hsu, C.-Y., Heimbuch, C. R., Armes, C. T., and Gates, B. C., *J. Chem. Soc. Chem. Commun.* 1645 (1992).
4. Yori, J. C., Luy, J. C., and Parera, J. M., *Appl. Catal.* **46**, 103 (1989).
5. Xu, B. Q., and Sachtler, W. M. H., *J. Catal.* **167**, 224 (1997).
6. Ebatini, K., Honno, H., Tanaka, T., and Hattori, H., *J. Catal.* **135**, 60 (1992).
7. Ebatini, K., Tanaka, T., and Hattori, H., *Appl. Catal. A* **102**, 79 (1993).
8. Iglesia, E., Soled, S. L., and Kramer, G. M., *J. Catal.* **144**, 238 (1993).
9. Arata, K., and Hino, M., *in* "Proceedings, 9th International Congress on Catalysis, Calgary, 1988" (M. J. Phillips and M. Ternan, Eds.), p. 1727. Chem. Institute of Canada, Ottawa, 1988.
10. Hino, M., and Arata, K., *J. Chem. Soc. Chem. Commun.* 1259 (1988).
11. Iglesia, E., Barton, D. G., Soled, S. L., Moseo, S., Baumgartner, J. E., Gates, W. E., Fuentes, G. A., and Meitzner, G. D., *in* "Proceedings, 11th International Congress on Catalysis, Baltimore, 1996" (J. W. Hightower, W. N. Delgass, E. Iglesia, and A. T. Bell, Eds.), Elsevier, Amsterdam, 1996; *Stud. Surf. Sci. Catal.* **101**, 533 (1996).
12. Larsen, G., Lotero, E., and Parra, R. D., *in* "Proceedings, 11th International Congress on Catalysis," *Stud. Surf. Sci. Catal.* **101**, 543 (1996).
13. Santiesteban, J. G., Vartuli, J. C., Han, S., Bastian, R. D., and Chang, C. D., *J. Catal.* **168**, 431 (1997).
14. Iglesia, E., Barton, D. G., Soled, S. L., Miseo, S., Baumgartner, J. E., and Gates, W. E., *in* "Abstracts of the 14th North American Meeting of the Catalysis Society, Snowbird Utah," p. T-45, 1995.
15. Larsen, G., and Petkovic, L. M., *J. Mol. Catal. A* **113**, 517 (1996).
16. Weisz, P. B., *Adv. Catal.* **13**, 137 (1962).
17. Guisnet, M., and Perot, G., *in* "Zeolites: Science and Technology" (F. R. Ribeiro, A. E. Rodrigues, L. D. Rollmann, C. Naccache, and M. Nijhoff, Eds.). NATO ASI Series, Series E: Applied Sciences-No. 80, Boston, 1984.
18. Ebitani, K., Konishi, J., and Hattori, H., *J. Catal.* **130**, 257 (1991).
19. Nakamura, I., Zhang, A., and Fujimoto, K., *Stud. Surf. Sci. Catal.* **109**, 325 (1997).
20. Hoang, D. L., and Lieske, H., *Catal. Lett.* **27**, 33 (1994).
21. Sermon, P. A., and Keryou, K. M., *Stud. Surf. Sci. Catal.* **112**, 251 (1997).
22. Khoobiar, S., *J. Phys. Chem.* **68**, 411 (1964).
23. Gerand, B., and Figlarz, M., *Stud. Surf. Sci. Catal.* **17**, 275 (1983).
24. Tauster, S. J., Fung, S. C., and Garten, R. L., *J. Amer. Chem. Soc.* **100**, 170 (1978).
25. Tauster, S. J., and Fung, S. C., *J. Catal.* **55**, 29 (1978).
26. Imelik, B., Naccache, C., Courdurier, G., Praliaud, H., Periaudeau, P., Gallezot, P., Martin, G. A., and Vedrine, J. C., (Eds.), *Stud. Surf. Sci. Catal.* **11**, 1 (1983).
27. Conner, W. C., Pajonk, G. M., and Teichner, S. J., *Adv. Catal.* **34**, 1 (1986).
28. Tournayan, L., Auroux, A., Charcosset, H., and Szymanski, R., *Adsorpt. Sci. Technol.* **2**, 55 (1985).
29. Yoshitake, H., and Iwasawa, Y., *J. Phys. Chem.* **96**, 1329 (1992).
30. Bitter, J. H., Seshan, K., and Lercher, J. A., *J. Catal.* **171**, 279 (1997).
31. Erre, R., and Fripiat, J. J., *Stud. Surf. Sci. Catal.* **17**, 285 (1983).
32. Farbotka, J. M., Garin, F., Girard, P., and Maire, G., *J. Catal.* **139**, 256 (1993).
33. Thomas, R., and Moulijn, J. A., *J. Mol. Catal.* **15**, 157 (1982).
34. Thomas, R., van Oers, E. M., de Beer, V. H. J., Madema, J., and Molujn, J. A., *J. Catal.* **76**, 241 (1982).
35. Wachs, I. E., Chersich, C. C., and Haedenbergh, J. H., *Appl. Catal.* **13**, 335 (1985).
36. Soled, S., Murrell, L. L., Wachs, I. E., McVicker, G. B., Sherman, L. G., Chan, S., Dispenziere, N. C., and Baker, R. T. K., *in* "ACS Symposium Series 279: Solid State Chemistry in Catalysis" (R. K. Grasselli and J. F. Brazdil, Eds.) p. 165. American Chemical Society, Washington, D.C., 1985.
37. Vannice, M. A., Boudart, M., and Fripiat, J. J., *J. Catal.* **17**, 359 (1970).
38. Benson, J. E., Kohn, H. W., and Boudart, M., *J. Catal.* **5**, 307 (1966).
39. Weitkamp, J., Jacobs, P. A., and Martens, J. A., *Appl. Catal.* **8**, 123 (1983).
40. Buchanan, J. S., Santiesteban, J. G., and Haag, W. O., *J. Catal.* **158**, 279 (1996).